Mechanisms of Oxidation of 2-Propanol by Polypyridyl Complexes of Ruthenium(III) and Ruthenium(IV)

Mark S. Thompson and Thomas J. Meyer*

Contribution from the Department of Chemistry, University of North Carolina, Chapel Hill, North Carolina 27514. *Received November 16, 1981*

Abstract: Kinetic and mechanistic studies have been carried out on the oxidation of 2-propanol to acetone in water by $Ru^{IV}(trpy)(bpy)O^{2+}$ (trpy is 2,2′,2″-terpyridine; bpy is 2,2′-bipyridine) and in acetonitrile by $Ru^{IV}(bpy)_2(py)O^{2+}$ (py is pyridine). The reactions proceed by oxidation of 2-propanol by Ru(IV) followed by a slower oxidation by the Ru(III) complexes $Ru(trpy)(bpy)OH^{2+}$ or $Ru(bpy)_2(py)OH^{2+}$. For the reactions: in water, $k_{IV}(25\ °C) = 6.7 \times 10^{-2}\ M^{-1}\ s^{-1}$, $\Delta H^{\ddagger} = 9 \pm 1$ kcal/mol, $\Delta S^{\ddagger} = -34 \pm 4$ eu, $k_H/k_D = 18 \pm 3$; in $[(CH_3)_2CHOH/(CD)_3)_2CDOH]$, $k_{III}(25\ °C) = 6 \times 10^{-5}\ M^{-1}\ s^{-1}$, $\Delta H^{\ddagger} = 19 \pm 2$ kcal/mol, $\Delta S^{\ddagger} = -12 \pm 6$ eu, $k_H/k_D = 2.7 \pm 1.4$. An ^{18}O-labeling experiment in 2-propanol and a spectral experiment in CH_3CN show that oxo transfer from the oxidant to the substrate does not occur. It is concluded that the most likely mechanism of oxidation for Ru(IV) is a concerted, two-electron hydride transfer from the α-C—H bond to Ru^{IV}=O with the oxo group acting as a lead-in atom to the Ru(IV) acceptor site. The Ru(III) reaction in water appears to occur by an initial one-electron, outer-sphere electron transfer. In acetonitrile there appears to be a change in mechanism for this reaction, apparently to a H-atom transfer, once again involving the α-C–H group. For this path: $k(25\ °C) = (8 \pm 2) \times 10^{-4}\ M^{-1}\ s^{-1}$, $\Delta H^{\ddagger} = 10 \pm 2$ kcal/mol, $\Delta S^{\ddagger} = -38 \pm 7$ eu, $k_H/k_D \geq 8$.

It has recently been shown that in polypyridyl complexes of ruthenium the +4 oxidation state is accessible at relatively low redox potentials by oxidation and loss of protons to give ruthenium(IV)–oxo complexes, as shown by the Latimer-type diagram in eq 1 (bpy is 2,2′-bipyridine).[1] Some remarkable features have

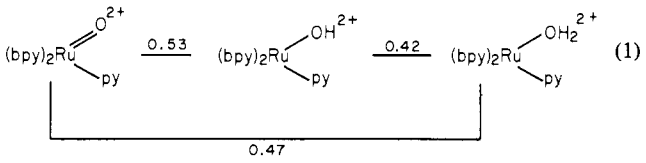

(1)

at pH 7

appeared in the redox chemistry of the pyridyl complexes and their 2,2′,2″-terpyridyl (trpy) analogues (eq 2). They include the

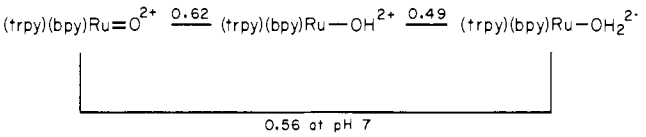

(2)

reversible reduction of NO_3^- to NO_2^- by $Ru(bpy)_2(py)OH_2^{2+}$ [2] and the electrocatalytic oxidation of a series of organic molecules (aromatic hydrocarbons, olefins, alcohols, aldehydes) based on $Ru(trpy)(bpy)O^{2+}$.[3] Mechanistic studies have revealed an oxygen atom transfer pathway in the oxidation of PPh_3 to $OPPh_3$ by $Ru(bpy)_2(py)O^{2+}$ [4] and the importance of proton-coupled electron transfer in the comproportionation reaction in eq 3 which has a solvent isotope effect of 16.1.[5]

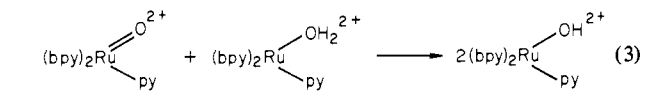

(3)

We have begun a series of kinetic and mechanistic studies based on the oxidation of organic molecules by $(bpy)_2(py)RuO^{2+}$ and $(trpy)(bpy)RuO^{2+}$. The results have already been of value to us in our attempts to design oxidation–reduction catalysts in a rational way based on the control of reactivity by synthetic modifications. However, the results of the mechanistic studies may be of even greater value from a fundamental point of view. The ruthenium complexes may offer an unparalleled view into metal complex based oxidation–reduction reactions both in terms of the identification of reaction pathways and in uncovering the intimate microscopic details associated with a particular pathway. That this is so arises from the chemical and physical properties of the complexes. (1) They are derived from a family of complexes whose simple electron-transfer chemistry is well understood.[6] (2) In contrast to most metal–oxo systems, the same primary structure in terms of coordination geometry is well-defined and maintained in a series of oxidation states. The structural response to changes in oxidation state is localized largely at the chemically active site, the $Ru{=}O/RuOH_2$ bond. (3) Given the spectral and redox properties of the complexes, it is relatively easy to obtain kinetic, thermodynamic, and mechanistic information. (4) The background synthetic chemistry is available for making relatively subtle changes and modifications in the complexes.

We report here on the results we have obtained for the oxidation of 2-propanol by $Ru(trpy)(bpy)O^{2+}$ and by its Ru(III) analogue $Ru(bpy)_2(py)OH^{2+}$ in aqueous solution. As a choice of substrate 2-propanol appeared to have several desirable features. (1) Our earlier catalytic studies had shown that 2-propanol is oxidized quantitatively to acetone.[3] (2) The reaction could involve either one or two electron-transfer steps. (3) 2-Propanol is convenient for both kinetic isotope and isotopic labeling experiments. (4) Results are available for the oxidation of 2-propanol and related alcohols by a series of other metal–oxo oxidants.[7]

Experimental Section

Materials. 2-Propanol from the Fisher Scientific Co. was fractionally distilled. Spectrograde acetonitrile was used as obtained from the Burdick and Jackson Laboratories. Sodium borodeuteride, 99.8% D_2O, and 99% atom D 2-propanol-d_8 were obtained from Aldrich Chemical Co. $H_2{}^{18}O$ (95% ^{18}O) was obtained from Mound Laboratory, OH. Lithium sulfate from the Mallinckrodt Chemical Co. was recrystallized once from

(1) Moyer, B. A.; Meyer, T. J. *J. Am. Chem. Soc.* **1978**, *100*, 3601; *Inorg. Chem.* **1981**, *20*, 436.
(2) Moyer, B. A.; Meyer, T. J. *J. Am. Chem. Soc.* **1979**, *101*, 1326–1328.
(3) Moyer, B. A.; Thompson, M. S.; Meyer, T. J. *J. Am. Chem. Soc.* **1980**, *102*, 2310–2312.
(4) Moyer, B. A.; Sipe, B. K.; Meyer, T. J. *Inorg. Chem.* **1981**, *20*, 1475–1480.
(5) Binstead, R. A.; Moyer, B. A.; Samuels, G. J.; Meyer, T. J. *J. Am. Chem. Soc.* **1981**, *103*, 2897–2899.
(6) (a) Keene, F. R.; Young, R. C.; Meyer, T. J. *J. Am. Chem. Soc.* **1977**, *99*, 2468. (b) Callahan, R. W.; Keene, F. R.; Meyer, T. J.; Salmon, D. J. *J. Am. Chem. Soc.* **1977**, *99*, 1064.
(7) (a) Barter, R. M.; Littler, J. S. *J. Chem. Soc. B* **1967**, 206. (b) Bartlett, P. D.; McCollum, J. D. *J. Am. Chem. Soc.* **1956**, *78*, 1441. (c) Strojny, E. J.; Iwamasa, R. T.; Frevel, L. K. *J. Am. Chem. Soc.* **1971**, *93*, 1171. (d) Westheimer, F. H.; Nicolaides, N. *J. Am. Chem. Soc.* **1949**, *71*, 25. (e) Spangler, M.; Saines, G.; Deno, N. *J. Am. Chem. Soc.* **1962**, *84*, 3295. See also ref 20 and 24.

0002-7863/82/1504-4106$01.25/0

boiling water and dried in a vacuum oven at 100 °C. Water was deionized and distilled from alkaline permanganate. All other solvents, simple salts, and other materials were obtained as reagent grade and used without further purification.

Preparations. The salts $[Ru(trpy)(bpy)OH_2](ClO_4)_2$,[8] $[Ru(trpy)(bpy)O](ClO_4)_2 \cdot 2H_2O$,[8] and $[Ru(bpy)_2(py)OH_2](ClO_4)_2$[1] were prepared by using literature procedures.

$[Ru(bpy)_2(py)^{18}O](ClO_4)_2$. A 20-mg sample of $[Ru(bpy)_2(py)OH_2](ClO_4)_2 \cdot H_2O$ was dissolved/suspended in 2 mL of $H_2{}^{18}O$ (95% ^{18}O) and the slurry stirred for 12 h. The solution was then oxidized by bubbling Br_2 gas through the slurry for 20 min, and the product was precipitated with 0.1 g of $NaClO_4$. The precipitate was collected on a frit and washed with 2 drops of ice-cold water. The extent of ^{18}O incorporation was ≥85%, based on the relative intensities of the ^{16}O and ^{18}O ν(Ru=O) stretching frequencies in the IR at 798 and 755 cm^{-1}.[9]

2-Deuterio-2-propanol ($(CH_3)_2CDOH$). A 1.00-g (2.38×10^{-2} mol) sample of sodium borodeuteride was dissolved in 30 mL of 0.1 M NaOH in a 100-mL round-bottom flask in an ice bath. A 7.0-mL (9.5×10^{-2} mol) sample of acetone was added dropwise to the solution, at all times keeping the solution temperature below 20 °C. When the addition of acetone was complete, 5 M sulfuric acid was added until the pH of the solution had reached between 1 and 2. A crude product was distilled off at 80.5 °C. The product was redistilled and its purity checked by proton NMR (% α-D ≥98%); yield, 2.8 mL (38%).

Sodium Isopropoxide ($(CH_3)_2CHONa$). A 5-g sample of sodium metal was stirred in 250 mL of 2-propanol until the solid metal had completely dissolved. The solution was filtered and the unreacted 2-propanol removed on a rotary evaporator. The crude white-tan product was dried for 1 h in a vacuum oven at 100 °C; yield, ~18 g.

O-Deuterated 2-Propanol ($(CH_3)_2CHOD$). A 18-g sample of sodium isopropoxide was added to 25 mL of deuterium oxide (99.8% atom D). A fraction boiling at 80.5 °C was collected by distillation. The product was fractionally distilled and the purity checked by proton NMR; yield, ~5 mL (30%; % O-D >85%).

Measurements. Routine UV–vis spectra were obtained on Bausch & Lomb 210 UV and Varian 634 spectrophotometers. Kinetic studies were monitored spectrophotometrically by using a Guilford Model 240 spectrophotometer. IR spectra were obtained with a Beckman 4250 IR spectrometer, and NMR spectra were obtained by using either a Perkin-Elmer R-24-B or a Varian XL-100 spectrometer.

NMR Spectra. All NMR measurements were made in D_2O/H_2O mixtures in a 5-mm tube and are referenced to Me_4Si as an external standard. Quantitative measurements were made by comparing the peak areas of a sample to be determined with the peak areas (with an appropriate factor correcting for differences in proton number) of weighed internal standards of either sodium acetate or sodium terephthalate.

Infrared Measurements. IR spectra of ruthenium complexes were obtained on sodium chloride plates as Nujol mulls. The IR spectrum of acetone prepared by oxidation of 2-propanol was obtained in neat 2-propanol in the ν(C=O) stretching region. The salt, $[Ru(trpy)(bpy)O](ClO_4)_2 \cdot 2H_2O$, which is slightly soluble in 2-propanol, was dissolved/suspended in neat 2-propanol, and the mixture was sonicated for 2 h. The slurry was allowed to stand for 24 h to allow the product salt $[Ru(trpy)(bpy)OH_2](ClO_4)_2$ to settle. The 2-propanol/acetone mixture was then pipetted off and the IR taken in NaCl solution cells.

Kinetic Measurements in Water. Rate data were obtained in a 1 cm cell by monitoring absorbance changes at 477 and 406 nm. The initial concentrations of $[Ru(trpy)(bpy)O]^{2+}$ were varied from 1×10^{-4} to 3×10^{-4} M. Solutions of the oxidant were generated by electrochemical oxidation of solutions containing $[Ru(trpy)(bpy)OH_2]^{2+}$ immediately prior to use. In separate experiments, it was shown that the electrochemical oxidation was quantitative with $n = 2.0$. Ionic strength variations were made between 0.05 and 3.02 M with lithium sulfate. Experiments at constant pH of 4.7, 6.8, and 8.9 were obtained by using 0.01 M acetate buffer, sodium phosphate, or sodium bicarbonate buffer, respectively.[10] The reactions were initiated by adding 2-propanol to thermostatted solutions. 2-Propanol concentrations were varied from 0.03 to 2.8 M. Except for solutions where O_2 was deliberately added, the solutions were purged with nitrogen and kept under a positive nitrogen pressure during the course of the kinetic runs. The method of kinetic analysis is somewhat complex and is described in the Appendix.

Stoichiometry. The stoichiometry of the net reaction in water, eq 4, was determined in two ways. In a previously reported experiment, acetone was shown to be the product of the $[Ru(trpy)(bpy)O]^{2+}$-catalyzed electrochemical oxidation of 2-propanol.[3] The acetone product was analyzed by vacuum distillation of the volatiles from the oxidized solution after roughly 250 catalytic turnovers. The acetone in the distillate was analyzed by using the $n \rightarrow \pi^*$ absorption band at 265 nm ($\epsilon = 16.4$)[11] and by ^1H NMR by comparing peak areas for acetone in the product solution before distillation with an added standard, acetate ion.

$$Ru(trpy)(bpy)O^{2+} + (CH_3)_2CHOH \rightarrow (CH_3)_2C{=}O + Ru(trpy)(bpy)OH_2^{2+} \quad (4)$$

A batch experiment was also performed in neat 2-propanol. A 0.24-g sample of $[Ru(trpy)(bpy)O](ClO_4)_2 \cdot 2H_2O$ was added to 0.5 mL of 2-propanol, the mixture allowed to stand for 24 h, and the IR spectrum taken with the spectrometer on absorbance mode. The intensity of the carbonyl stretch was compared to a calibration plot from prepared standards of acetone in 2-propanol.

Kinetics in Acetonitrile Using $[Ru(bpy)_2(py)O]^{2+}$ as Oxidant. In an attempt to ascertain the role of solvent in the reaction, the kinetics were studied in acetonitrile. For the studies in acetonitrile, $[Ru(bpy)_2(py)O]^{2+}$ was used as oxidant because it is stable on the time scale of hours in acetonitrile while the stability of the terpyridine complex is limited, apparently because of oxidation of the solvent or of impurities in the solvent. The reactions were carried out by dissolving $[Ru(bpy)_2(py)O]^{2+}$ in acetonitrile and adding 2-propanol by syringe. The 2-propanol concentration was varied between 0.1 M and 0.8 M in the kinetics runs. No attempt was made to deoxygenate the solutions. Absorbance changes with time were observed at 448 nm, which is an isosbestic point between the spectra of $Ru(bpy)_2(py)OH_2^{2+}$ and $Ru(bpy)_2(py)NCCH_3^{2+}$. The advantage of making observations at the isosbestic point is that in acetonitrile, the aquo complex if formed undergoes solvolysis to give the acetonitrile complex. By monitoring at the isosbestic point, even if the solvolysis reaction plays a role, it will leave the absorbance vs. time data for the oxidation unaffected.

In order to determine the nature of the initial Ru(II) product, the reaction between $Ru(bpy)_2(py)O^{2+}$ and 2-propanol was quenched by the addition of 1 mL of 64% hydrazine when the Ru(IV) was approximately 75% reduced and the spectrum of the resulting solution was scanned rapidly in the visible region.

Results

Stoichiometry Measurements. The stoichiometry of the reaction between 2-propanol and $Ru(trpy)(bpy)O^{2+}$ has been measured in two ways. The electrocatalytic experiments described in a recent paper[3] gave 95% and 87% yields of acetone when analyzed by UV–vis and NMR, respectively. There is no evidence for other products and the 2-propanol to acetone conversion appears to be quantitative. The yield in the electrocatalytic reaction was based on the total number of coulombs passed which indicated ~250 2-propanol to acetone conversions per ruthenium complex and suggested the stoichiometry shown in reaction 4. The stoichiometry of the 2-propanol oxidation was also investigated in neat 2-propanol and the yield of 2-propanol in the stoichiometric reaction as analyzed by IR was 1:1 within experimental error.

Spectral Changes and Search for Intermediates. An aqueous solution containing $Ru(trpy)(bpy)O^{2+}$ was made 0.01 M in 2-propanol, and its absorption spectrum was scanned repeatedly between 350 and 700 nm. As shown in Figure 1, in the initial stages of the reaction an isosbestic point appears at 363 nm. After several spectral runs the isosbestic point at 363 nm had disappeared and was replaced by one at 406 nm which remained for the duration of the experiment. The isosbestic points exactly match those which appear in the electrochemical reduction of Ru(IV) to Ru(III) and of Ru(III) to Ru(II) in water.[8] The observed spectral changes are consistent with the initial reduction of $Ru(trpy)(bpy)O^{2+}$ to $Ru(trpy)(bpy)OH^{2+}$ perhaps via eq 5 and 6

$$Ru(trpy)(bpy)O^{2+} + (CH_3)_2CHOH \rightarrow Ru(trpy)(bpy)OH_2^{2+} + (CH_3)_2C{=}O \quad (5)$$

$$Ru(trpy)(bpy)O^{2+} + Ru(trpy)(bpy)OH_2^{2+} \underset{(25\ °C)}{\overset{K = 200}{\rightleftharpoons}} 2Ru(trpy)(bpy)OH^{2+} \quad (6)$$

$$2Ru(trpy)(bpy)O^{2+} + (CH_3)_2CHOH \rightarrow 2Ru(trpy)(bpy)OH^{2+} + (CH_3)_2C{=}O \quad (7)$$

(8) Thompson, M. S.; Meyer, T. J., submitted for publication.
(9) Moyer, B. A. Ph.D. Dissertation, University of North Carolina, Chapel Hill, 1979.
(10) Weast, R. C., Ed. "Handbook of Chemistry and Physics"; CRC Press: Cleveland, OH, 1976.
(11) "DMS UV Atlas of Organic Compounds"; Plenum Press: New York, 1966; Vol. II.

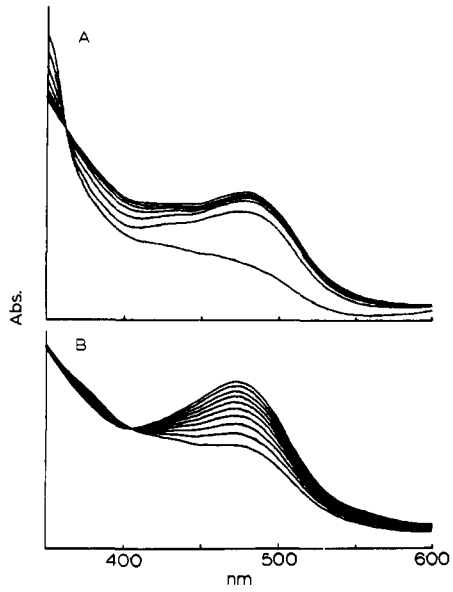

Figure 1. Successive spectral scans observed during the reduction of $Ru(trpy)(bpy)O^{2+}$ by 2-propanol (0.01 M) in pH 6.8 phosphate buffer at 25 °C in a 1-cm cell: (A) the first stage of reaction, absorbance increases occur with successive spectral scans; (B) the second stage, absorbance increases also occur with time.

followed by slower reduction of $Ru(trpy)(bpy)OH^{2+}$ to $Ru(trpy)(bpy)OH_2^{2+}$, eq 8. The comproportionation reaction in eq

$$2Ru(trpy)(bpy)OH^{2+} + (CH_3)_2CHOH \rightarrow 2Ru(trpy)(bpy)OH_2^{2+} + (CH_3)_2CO \quad (8)$$

6 is known to be rapid[5] on the time scale for the 2-propanol oxidation (see below). In the latter stages of the reaction shown in Figure 1, the Ru(IV) complex is present at low concentrations because of the magnitude of the comproportionation constant. A significant point which arises from the spectral study is that if there are any intermediates present, they do not build up to appreciable concentrations or are too short-lived to be seen spectrophotometrically.

Kinetics Data. The kinetic analysis used to treat the rate data is presented in the Appendix. It is based on the observation of transient absorbance changes and yields rate constants for the oxidation of 2-propanol by both Ru(IV) and Ru(III). Rate constants were obtained from kinetic traces taken at 477 and 406 nm at constant temperature. For the oxidation by Ru(IV) the reaction is first order in ruthenium and first order in 2-propanol as shown by varying the 2-propanol concentration over the range 0.03–2.8 M. At 25.3 °C for the oxidation by Ru(IV), $k_{IV} = (6.7 \pm 0.7) \times 10^{-2}$ M^{-1} s^{-1}. As can be seen from the data in Table I, and other data not represented there, k_{IV} is not sensitive to the presence of oxygen in an air-saturated solution (experiment 6), to variations in ionic strength over the range 0.05–3.0 M (experiments 1–5), nor to changes in pH over the range 4.9–8.9 (experiments 1–3).

At 25 °C the two reactions are sufficiently well separated that the Ru(IV) reaction can be studied separately under simple pseudo-first-order conditions. When followed at 406 nm, which is an isosbestic point for Ru(II) and Ru(III) (note Figure 1), only the first reaction is observed experimentally. Rate constants obtained this way are in fairly good agreement with values obtained from the more complex analysis (experiment 9 in Table I), but the majority of our data were obtained from the complete analysis since it appeared to give more accurate values. The rate constant for oxidation by Ru(III) is less well-defined than k_{IV} because the oxidation by Ru(III) becomes important in relative terms only near the end of the reaction (after ~5 half-lives) where the composition of the solution is largely Ru(II) and Ru(III). Because of the small contribution by Ru(III) to the total oxidation, it is not possible to assess independently the stoichiometry of the oxidation by Ru(III). However, it is quite clear that there is an intrinsic path for the oxidation of 2-propanol by Ru(III), and it is of value in making comparisons with the k_{IV} path as discussed later.

Table I. Representative Rate Constant Data for the Oxidation of 2-Propanol by $Ru(trpy)(bpy)O^{2+}$ (k_{IV}) and by $Ru(trpy)(bpy)OH^{2+}$ (k_{III}) in Water at 25.3 ± 0.1 °C[a]

expt	$10^2 k_{IV}$,[b] M^{-1} s^{-1}	$10^5 k_{III}$, M^{-1} s^{-1}	μ, M	pH
1	6.3	6.0 ± 1.5	0.32	4.9
2	6.7	5.5 ± 0.15	0.32	6.8
3	6.7	18 ± 4	0.32	8.9
4	6.7	9.5 ± 2.5	1.52	6.8
5	6.9	1.5 ± 0.3	3.02	6.8
6	6.7[c]		0.32	6.8
7		9.0 ± 3.0	0.32	6.8
8		6.5 ± 1.0[c]	0.32	6.8
9	7.6		0.20	6.8

[a] In deaerated solutions unless otherwise indicated; ionic strength was maintained with Li_2SO_4. [b] Estimated error is ±0.7. [c] Air-saturated solution.

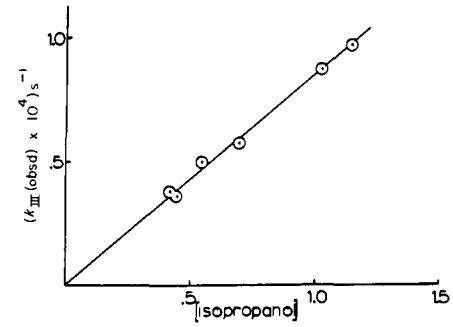

Figure 2. Plot of $k_{III}(obsd) \times 10^4$ vs. 2-propanol concentration at 25.3 ± 0.10 °C showing the first-order dependence on 2-propanol (μ = 0.32 M). Note from the stoichiometry in eq 9 and 10 that $k_{III}(obsd) = 2k_{III}$.

From the rate data, the reaction between Ru(III) and 2-propanol is first order in both metal complex and alcohol. Note Figure 2. Since Ru(III) is a one-electron oxidant, the net reaction in eq 8 must occur stepwise as suggested by the reactions in eq 9 and 10. The rate constant for the Ru(III) path can also be

$$Ru(trpy)(bpy)OH^{2+} + (CH_3)_2CHOH \xrightarrow{k_{III}} (CH_3)_2\dot{C}OH + Ru(trpy)(bpy)OH_2^{2+} \quad (9)$$

$$Ru(trpy)(bpy)OH^{2+} + (CH_3)_2\dot{C}OH \xrightarrow{fast} (CH_3)_2C{=}O + Ru(trpy)(bpy)OH_2^{2+} \quad (10)$$

obtained from simple first-order kinetic plots (ln (Δ(absorbance)) vs. time) after 5 half-lives where the direct reaction involving Ru(III) dominates the observed absorbance change (Figure 3). Here there was only fair agreement with rate constant values obtained from the more detailed analysis. As developed below in the Discussion, the difficulty in obtaining k_{III} directly lies in separating the intrinsic path involving Ru(III) from an indirect path involving Ru(IV). The indirect path, which dominates the middle stages of the reaction, involves disproportionation of Ru(III) to give Ru(IV) and Ru(II) (the reverse of eq 6) followed by the oxidation by Ru(IV) in eq 4. The indirect path is competitive with the direct oxidation by Ru(III) because $k_{IV} >> k_{III}$.

In aerated solutions k_{IV} is unaffected by the presence of O_2, but k_{III} decreases by 30% (note experiments 7 and 8 in Table I). The decrease is expected from eq 9 and 10 based on the effect on the stoichiometry of eq 7 of competitive scavenging for the 2-propanol radical between O_2 and $Ru(trpy)(bpy)OH^{2+}$.

From the data in Table I, k_{III} is dependent both on ionic strength and on pH in the range 4.9–8.9. A plot of log k_{III} vs. the extended ionic strength function $\mu^{1/2}/(1 + \mu^{1/2})$[12] is linear with slope 1.5 ± 0.5 and intercept 0. At pH 9, k_{III} takes a sharp upward turn

(12) Pearson, R. G.; Frost, A. A. "Kinetics and Mechanisms"; Wiley: New York, 1961.

Table II. Kinetic Isotope Effects in H_2O or D_2O at 25.3 °C (μ = 0.32 M with Li_2SO_4, pH 6.8)

expt	substrate	10^2k_{IV}, M^{-1} s^{-1}	10^4k_{III}, M^{-1} s^{-1}	k_H/k_D(IV)	k_H/k_D(III)	medium
1	$(CH_3)_2CHOH$	6.7 ± 0.7	1.1 ± 0.3	1.0	1.0	H_2O
2	$(CD_3)_2CDOH$	0.37 ± 0.04	4.4 ± 1	18 ± 3	2.7 ± 1.4	H_2O
3	$(CH_3)_2CDOH$	1.3 ± 0.2	6.0 ± 2	5.2 ± 0.8	2.0 ± 1.0	H_2O
4	$(CH_3)_2CHOD$	6.0 ± 0.6	1.8 ± 0.6	1.1 ± 0.1	0.6 ± 0.6	D_2O
5	$(CD_3)_2CHOH$			3.5 ± 0.6[a]	1.4 ± 0.7[a]	H_2O

[a] Values calculated from the total isotope effect in experiment 2 and the results in experiment 3.

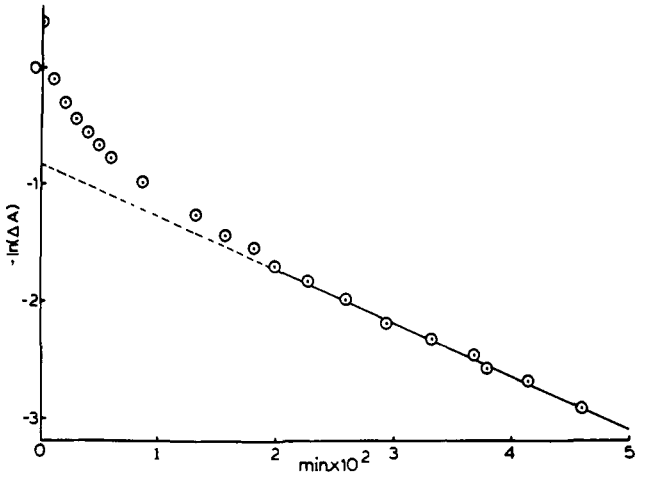

Figure 3. Plot of ln (absorbance change) vs. time at 477 nm for the reduction of Ru(trpy)(bpy)O^{2+} by 2-propanol in water. The linear region late in the reaction corresponds to the region where direct reduction of Ru(trpy)(bpy)OH^{2+} dominates the reaction.

(experiment 3 in Table I). We have not studied the kinetics of the reaction in detail at higher pH values, in part, because of the long-term instability of the Ru(III) and Ru(IV) complexes under these conditions.[13] However, it is clear that at higher pHs, the Ru(III) oxidation of 2-propanol is dominated by a pathway or pathways which have at least an inverse acid dependence.

For the acid independent pathways for both k_{III} and k_{IV}, activation parameters were determined from the slopes and intercepts of plots of ln (k/T) vs. $1/T$ over the temperature range 25–41 °C (Figure 4). The points shown in Figure 4 represent average values of multiple (3 or greater) kinetic runs. For the oxidation by Ru(IV), $\Delta H^{\ddagger}$ = 9 ± 1 kcal/mol and $\Delta S^{\ddagger}$ = −34 ± 4 eu. For the oxidation by Ru(III), $\Delta H^{\ddagger}$ = 19 ± 2 kcal/mol and $\Delta S^{\ddagger}$ = −3 ± 6 eu.

Kinetic Isotope Effects. A summary of rate constants obtained for the oxidation of various deuterated forms of 2-propanol by Ru(trpy)(bpy)O^{2+} and Ru(trpy)(bpy)OH^{2+} at 25.3 °C are summarized in Table II. Clearly worth noting are the rather sizeable total and α- and β-C–H isotope effects associated with the oxidation by Ru(IV). It should be noted that for experiments in D_2O with Ru(III) both the alcohol and the complex Ru(trpy)(bpy)-OD^{2+} are O deuterated.

^{18}O Labeling. A reaction between 2-propanol and Ru-$(bpy)_2py^{18}O^{2+}$ (≥85% ^{18}O in Ru=O) in neat 2-propanol was carried out as described in the Experimental Section. The extent of ^{18}O transfer was determined by comparing peak areas for the $\nu(C{=}{}^{16}O)$ = 1710 cm^{-1} and $\nu(C{=}{}^{18}O)$ = 1670 cm^{-1} bands. A comparison between peak areas assuming the same oscillator strengths for the two vibrations showed that the degree of ^{18}O incorporation into the acetone product was ≤10%. The labeling result shows that the oxygen atom in the acetone product does not originate as the oxo group of the oxidant within the uncertainty of the experiment.

Kinetics and Labeling Studies in Acetonitrile. The oxidation of 2-propanol by Ru$(bpy)_2(py)O^{2+}$ and Ru$(bpy)_2(py)OH^{2+}$ was studied in acetonitrile. From spectral changes observed after mixing the two reagents the basic oxidation mechanism appears

(13) Simmons, M., unpublished results.

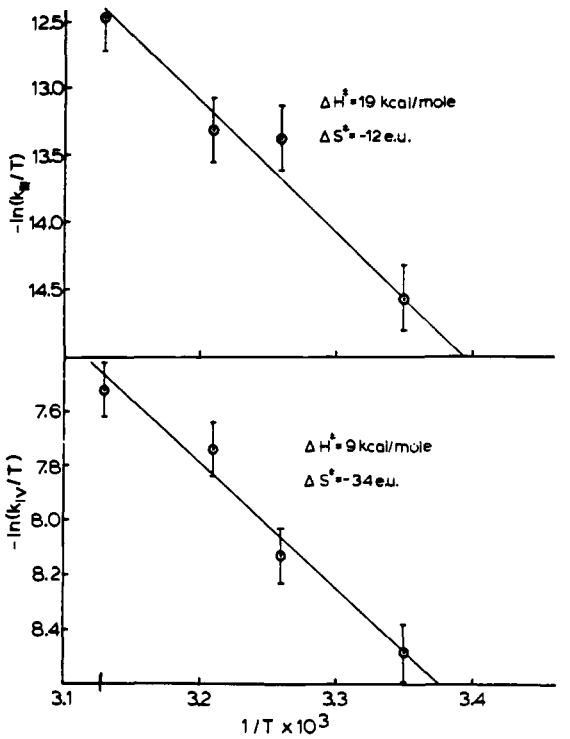

Figure 4. Plots of ln k/T vs. $1/T$ for the oxidation of 2-propanol in water by Ru(trpy)(bpy)O^{2+} (bottom) and Ru(trpy)(bpy)OH^{2+} (top).

to be the same in both solvents. In acetonitrile k_{IV} is decreased and k_{III} increased compared to water, the middle stage reaction involving the initial disproportionation of Ru(III) followed by oxidation by Ru(IV) is relatively unimportant, and reliable values for k_{IV} and k_{III} could be obtained by simply treating the Ru(IV) and Ru(III) reductions as successive, pseudo-first-order reactions.

There is an experimental complication associated with the reaction in acetonitrile. Following reduction to Ru(II), solvolysis occurs to give the acetonitrile complex Ru$(bpy)_2(py)CH_3CN^{2+}$ (λ_{max} 440 nm (ϵ 8400)).[4] Spectral complications in the kinetic studies arising from reaction 11 were circumvented by using an isosbestic point for the aquo–acetonitrile conversion (448 nm) as the monitoring wavelength.

$$Ru(bpy)_2(py)H_2O^{2+} + CH_3CN \xrightarrow[T = 24.4\ ^\circ C]{k = 1.5 \times 10^{-3}\ s^{-1}} Ru(bpy)py(CH_3CN)^{2+} + H_2O \quad (11)$$

For the oxidation of 2-propanol by Ru(IV) and Ru(III) rate constants at 24.4 ± 0.1 °C obtained as described above were k_{IV} = (8.7 ± 0.9) × 10^{-3} M^{-1} s^{-1} and k_{III} = (4 ± 1) × 10^{-4} M^{-1} s^{-1}.

From the results of experiments at varying 2-propanol concentrations, a plot of k_{IV}(obsd) vs. [2-propanol], where k_{IV}(obsd) = k_{IV}[2-propanol], is linear with a zero intercept within experimental error, as expected. However, for k_{III} a plot of k_{III}(obsd) vs. [2-propanol] gives a nonzero intercept of 5 × 10^{-5} s^{-1}. The intercept appears to correspond to an intrinsic instability of Ru-$(bpy)_2(py)OH^{2+}$ in acetonitrile either through a reaction with solvent or with impurities in the solvent.

It is difficult to make detailed comparisons between the two solvents because different, if closely related oxidants are involved

Table III. Kinetic Isotope Effects in Acetonitrile at 24.8 ± 0.1 °C

expt	substrate	$10^3 k_{IV}$, M^{-1} s^{-1}	$10^4 k_{III}$, M^{-1} s^{-1}	k_H/k_D(IV)	k_H/k_D(III)
1	$(CH_3)_2CHOH$	8.7 ± 0.9	8.2 ± 2	1.0	1.0
2	$(CD_3)_2CDOD$	0.67 ± 0.07	≤1.0	13 ± 2	≥8
3	$(CH_3)_2CHOD$	6.0 ± 0.6	6.2 ± 1.5	1.5 ± 0.3	1.3 ± 0.4

Table IV. Summary of Kinetics Data in Water and Acetonitrile at 25 °C

oxidant	medium	k, M^{-1} s^{-1}	$\Delta H^{\ddagger}$, kcal/mol	$\Delta S^{\ddagger}$, eu	$k_H/k_D((CD_3)_2CDOD)$
$Ru(trpy)(bpy)O^{2+}$	H_2O[a]	$(6.7 \pm 0.7) \times 10^{-2}$	9 ± 1	−34 ± 4	18 ± 3
$Ru(bpy)_2(py)O^{2+}$	CH_3CN	$(8.7 \pm 0.9) \times 10^{-3}$	8 ± 1	−42 ± 5	13 ± 2
$Ru(trpy)(bpy)OH^{2+}$	H_2O[a]	$(6 \pm 1) \times 10^{-5}$ [b]	19 ± 2	−12 ± 6	2.7 ± 1.4
$Ru(bpy)_2(py)OH^{2+}$	CH_3CN	$(4 \pm 1) \times 10^{-4}$ [b,c]	10 ± 2	−38 ± 7	≥8

[a] At pH 6.8, $\mu = 0.32$ M with Li_2SO_4. [b] The value cited for k_{III} assumes that the reaction stoichiometry is as in eq 13. [c] The kinetics data in acetonitrile were obtained in an aerated solution so that $2 \times 10^{-4} < k_{III} \leq 4 \times 10^{-4}$ M^{-1} s^{-1}.

and redox potentials are not available in acetonitrile. However, the decrease in the ratio of k_{IV} to k_{III} in going from the terpyridine complex in water ($k_{IV}/k_{III} = 1200$) to the pyridine couple in acetonitrile ($k_{IV}/k_{III} = 20$) is certainly worth noting.

The kinetics of oxidation of perdeuterio and 2-propanol-*O*-*d* were also studied in acetonitrile, and the results appear in Table III. A reliable value could not be obtained for the oxidation of $(CD_3)_2CDOD$ by $Ru(bpy)_2(py)OH^{2+}$ at a reasonable 2-propanol concentration because the reaction is slow and the observed rate constant was not appreciably above the background reaction of the complex with the medium mentioned above.

Activation parameters for the reactions of 2-propanol with Ru(III) and Ru(IV) were obtained from plots of ln (k/T) vs. $1/T$ over the temperature range 25–42 °C. The results obtained were as follows: for k_{IV}, $\Delta H^{\ddagger} = 8 \pm 1$ kcal/mol and $\Delta S^{\ddagger} = -42 \pm 5$ eu; for k_{III}, $\Delta H^{\ddagger} = 10 \pm 2$ kcal/mol and $\Delta S^{\ddagger} = -38 \pm 7$ eu.

The nature of the initial ruthenium product following reduction of $Ru(bpy)_2(py)O^{2+}$ in acetonitrile also offers some mechanistic insight. As mentioned previously, oxo transfer does not occur as a dominant pathway as shown by the ^{18}O-labeling experiment. The labeling experiment is reinforced by the appearance of $Ru(bpy)_2pyOH^{2+}$ as an intermediate in the reaction in acetonitrile. If oxo transfer had occurred, the initially observed Ru product would have had to have been $Ru(bpy)_2(py)CH_3CN^{2+}$, via eq 12.

$$Ru(bpy)_2(py)O^{2+} + (CH_3)_2CHOH + CH_3CN \rightarrow (CH_3)_2CO + H_2O + Ru(bpy)_2(py)CH_3CN^{2+} \quad (12)$$

The acetonitrile complex is stable in the presence of $Ru(bpy)_2(py)O^{2+}$ on the time scale of the experiments described here, and with the trace water in the solution, aquation of the acetonitrile complex does not occur. In an attempt to make the observation quantitative, the reaction between $Ru(bpy)_2pyO^{2+}$ and isopropanol was allowed to proceed through 2 half-lives. After 2 half-lives the solution contained mainly $Ru(bpy)_2(py)OH^{2+}$ and some $Ru(bpy)_2(py)OH_2^{2+}$. A small amount (~1 μL) of hydrazine was added to the solution. In small amounts hydrazine leads to the rapid, quantitative reduction of Ru(IV) and Ru(III) to $Ru(bpy)_2(py)OH_2^{2+}$ and the Ru(II) complex has an intense visible absorption band in acetonitrile (λ_{max} 472 nm). Following the reduction, spectral analysis using known extinction coefficients for the two complexes in acetonitrile indicated that the product distribution was ~80% aquo complex and ~20% acetonitrile complex. The appearance of some acetonitrile complex is expected because of solvolysis of $Ru(bpy)_2(py)H_2O^{2+}$ formed from both the hydrazine and 2-propanol reductions of $Ru(bpy)_2(py)OH^{2+}$. Although not quantitative, the result supports the suggestion that oxygen transfer from Ru(IV) to 2-propanol does not occur appreciably for the reaction in acetonitrile.

Discussion. The stoichiometry of the oxidation of 2-propanol by $Ru(trpy)(bpy)O^{2+}$ is as shown in eq 4. Spectral studies and the agreement of the absorbance vs. time data with the kinetic treatment derived in the Appendix show that the oxidation occurs in three distinct stages. In the first stage, Ru(IV) is reduced to Ru(III) as previously mentioned. In the second stage, Ru(III) is reduced to Ru(II) but the mechanism still largely involves Ru(IV). There is an initial disproportionation into Ru(II) and Ru(IV), followed by the oxidation of 2-propanol by Ru(IV) (eq 13). The reason that the reaction through Ru(IV) is still important at this stage is the fact that k_{IV} is almost 3 orders of magnitude larger than k_{III}. Although the dominant Ru species in solution is the +3 oxidation state, an appreciable fraction of the total reaction still occurs through Ru(IV) because of its higher intrinsic reactivity. The example cited in reaction 13 is that of the pyridyl complex since the rate constant data are available for that system from equilibrium and stopped-flow measurements,[5] however, the properties of the trpy–bpy and bis/bpy–py systems are very similar.[8]

$$2Ru(bpy)_2(py)OH^{2+} \underset{k = 1.4 \times 10^5\ M^{-1}\ s^{-1}}{\overset{k = 1.9 \times 10^4\ M^{-1}\ s^{-1}}{\rightleftharpoons}} Ru(bpy)_2(py)O^{2+} + Ru(bpy)(py)OH_2^{2+} \quad (13)[5]$$

The third stage of the reaction involves the intrinsic oxidation of isopropanol by $Ru(trpy)(bpy)OH^{2+}$. From the rate constant data in water at 25 °C, oxidation of 2-propanol by Ru(III) is slower by a factor of 1200 than oxidation by Ru(IV), and the third stage of the reaction accounts for only a small part of total oxidation. Consequently, the stoichiometry results apply only to the oxidation by Ru(IV). However, it is reasonable that the stoichiometry of the reaction with Ru(III) is that shown in eq 14 and we have assumed in it the calculation of rate constants.

$$2Ru(trpy)(bpy)OH^{2+} + (CH_3)_2CHOH \rightarrow 2Ru(trpy)(bpy)OH_2^{2+} + (CH_3)_2CO \quad (14)$$

Oxidation Mechanisms in Water. There are several levels at which to consider the oxidation mechanism(s). The first is a classification of the redox processes as involving the transfer of one or two electrons in the rate-determining step. A second level of consideration concerns the structural details of the oxidation pathway, including the identification of intermediates. The final and most sophisticated level of analysis involves elucidation of the microscopic details of the reaction, including the role of electronic coupling and of selected molecular vibrations which define the reaction energy surface.

In order to facilitate comparisons, the various kinetic parameters describing the k_{III} and k_{IV} pathways are collected in Table IV.

Redox Step for Ru(trpy)(bpy)OH^{2+} in Water. Of the two oxidants, the more straightforward case to consider is Ru(III). The mechanism must involve a one-electron-transfer step given the one-electron nature of the oxidant. The radical nature of the reaction in eq 9 is supported by the dependence of the observed rate constant on oxygen. The decrease in k_{obsd} in an aerated solution is consistent with capture of the intermediate organic radical by oxygen before oxidation by a second Ru(III) can occur.

The details of the one electron step in the reaction in eq 9 are unclear. They could involve initial outer-sphere electron transfer followed by rapid proton loss as depicted in reaction 15, a hydrogen

$$Ru(trpy)(bpy)OH^{2+} + (CH_3)_2CHOH \rightarrow Ru(trpy)(bpy)OH^{+} + (CH_3)_2CHOH^{+} \xrightarrow{\text{(rapid)}} Ru(trpy)(bpy)OH_2^{2+} + (CH_3)_2COH \quad (15)$$

atom transfer involving the α-C–H bond, as in eq 16, or a hydrogen

$$Ru(trpy)(bpy)OH^{2+} + (CH_3)_2CHOH \rightarrow Ru(trpy)(bpy)OH_2^{2+} + (CH_3)_2\dot{C}OH \quad (16)$$

atom transfer or proton-coupled electron transfer[5] involving the hydroxyl group followed by rearrangement to the more stable carbon-based radical, eq 17. The pathway of eq 17 has been identified for the one-electron-transfer reaction shown in eq 18,

$$Ru(trpy)(bpy)OH^{2+} + (CH_3)_2CHOH \rightarrow Ru(trpy)(bpy)OH_2^{2+} + (CH_3)_2\dot{C}HO \xrightarrow{\text{(rapid)}} (CH_3)_2\dot{C}OH \quad (17)$$

$$Ru(trpy)(bpy)OH^{2+} + Ru(bpy)_2pyOH_2^{2+} \rightarrow Ru(trpy)(bpy)OH_2^{2+} + Ru(bpy)_2pyOH^{2+} \quad (18)$$

as well as for the comproportionation reaction in eq 13 and both are characterized by abnormally large solvent kinetic isotope, k_{H_2O}/k_{D_2O}, effects.[5,14] Microscopically, the characteristic features of this pathway appear to be a relatively weak electronic coupling between the electron donor and acceptor sites and proton transfer by vibrational tunneling.[5,14] The lack of a significant kinetic isotope effect upon OH deuteration of 2-propanol (Table II) argues against this pathway.

We have no substantial evidence for choosing between the mechanisms of equations 15 and 16, but the following observations should be noted. (1) Nearly all the relatively small k_H/k_D isotope effect has its origin in the C–H bond (Table II). If the reaction involves outer-sphere electron transfer, the contribution to the vibrational barrier from intramolecular vibrations must be dominated by the C–H mode. (2) The ionic strength acceleration observed for the reaction is consistent with the formation of like charges in the activation process and therefore with the outer-sphere reaction in eq 15. It should be noted that under the same conditions there is no ionic strength effect on the rate constant k_{IV}. (3) One thermodynamic disadvantage of the outer-sphere mechanism arises from the acid–base character of the initially formed products. The formation of the strong acid $(CH_3)_2CHOH^{+}$ [15] and strong base $Ru(bpy)_2(py)OH^{+}$ [1] adds to the activational requirements of the reaction. In part, this may be the origin of the rate acceleration at higher pH which is reminiscent of the situation found in the oxidation of alcohols by permanganate and which has been attributed to initial loss of a proton from the alcohol followed by oxidation of the alkoxide ion.[16] We have been unable to document the base-catalyzed path in detail partly because at higher pH the oxidant is unstable.[13] (4) The α-C–H bond kinetic isotope effect in water (Table II) is very small compared to other cases where C–H hydrogen abstraction is known or thought to occur.[17] In fact, the activation parameters for the reaction are consistent with an outer-sphere electron-transfer reaction where electrostatic effects do not play a role (note from Table IV that $\Delta S^{\ddagger} = 12 \pm 6$ eu) and for which a significant intramolecular vibrational barrier exists from the $(CH_3)_2CHOH^{+/0}$ couple.

The energetics of the Ru(III) oxidation are shown below where redox potentials for the organic couples were taken from the estimates given by Henglein et al.[15]

$$Ru^{III}(trpy)(bpy)OH^{2+} + (CH_3)_2CHOH \rightarrow Ru^{II}(trpy)(bpy)OH_2^{2+} + (CH_3)_2\dot{C}OH$$

$$\Delta G = -13.5 \text{ kcal/mol}$$

$$Ru^{III}(trpy)(bpy)OH^{2+} + (CH_3)_2\dot{C}OH \rightarrow Ru^{II}(trpy)(bpy)OH_2^{2+} + (CH_3)_2CO$$

$$\Delta G = -47 \text{ kcal/mol}$$

The Redox Step for Ru(trpy)(bpy)O^{2+} in Water. The one-electron nature of the oxidation of 2-propanol by Ru(III) provides a useful starting point for discussing the oxidation by Ru(IV). In comparing their properties as oxidants, Ru(IV) is a slightly stronger oxidant than Ru(III) ($\Delta E = 0.14$ V) over the pH range 2–9. The presence of oxygen has no effect on the observed Ru(IV) rate constant, arguing against the presence of discrete separated radicals in solution, although not ruling out sequential one-electron transfers. If the reaction were initiated by one-electron steps such as those discussed in the previous section, oxygen could only intervene if the resulting one-electron intermediates can diffuse apart before a second electron transfer occurs. Since oxygen is not seen to interfere, it follows from the scheme in eq 19 that a

$$Ru(trpy)(bpy)O^{2+} + (CH_3)_2CHOH \rightarrow Ru(trpy)(bpy)OH^{2+}, (CH_3)_2\dot{C}OH$$

$$\swarrow k_{-D} \qquad \downarrow k_{et}$$

$$Ru(trpy)(bpy)OH^{2+} + (CH_3)_2\dot{C}OH \qquad Ru(trpy)(bpy)OH_2^{2+} + (CH_3)_2C{=}O \quad (19)$$

necessary condition is that $k_{et} > k_{-D}$. The latter condition allows certain restrictions to be placed on the magnitude of k_{et}. k_{-D} can be estimated from

$$k_{-D} = k_D/K_A$$

where K_A is the equilibrium constant for formation of the association complex between the reagents following the initial one-electron-transfer step. k_D is the diffusion-limited rate constant for formation of the association complex. It is given by

$$k_D = \frac{2RT}{3000\eta}\left(2 + \frac{r_A}{r_B} + \frac{r_B}{r_A}\right)$$

where r_A and r_B are the molecular radii of the reagents, η is the solution viscosity, and the Stokes–Einstein equation has been used to calculate diffusion coefficients for the reagents.[19] Using $\eta = 10 \times 10^{-3}$ P for water, average molecular radii of 6.5 and 3.0 Å for the Ru complex and 2-propanol, respectively, and $K_A = 2$ (note below) gives $k_{et} > k_{-D} = 3\text{–}4 \times 10^9$ s^{-1}.

Although Ru(trpy)(bpy)O^{2+} and Ru(trpy)(bpy)OH^{2+} have comparable strengths as oxidants and related structures, the available evidence strongly suggests that the oxidations occur by different mechanisms. (1) There is no ionic strength dependence on k_{IV}. (2) The isotope effects for the two reactions are strikingly different. (3) The pattern of activation parameters is also very different for the two reactions, with the Ru(IV) reaction having a small $\Delta H^{\ddagger}$ and a large, negative $\Delta S^{\ddagger}$.

The pattern of activation parameters for the Ru(IV) reaction is consistent with a more complex mechanism, perhaps involving specific vibrational and orientational demands or solvent ordering. the same pattern in activation parameters is observed for the oxidation of secondary alcohols by RuO_4.[20] For the latter oxidant, it has been suggested that the mechanism involves a two-electron mechanism by hydride transfer.

A number of lines of evidence suggest that the oxidation of 2-propanol and other organic substances by Ru(trpy)(bpy)O^{2+} also involves a two-electron transfer. They include the following. (1) The differences in isotope effects and activation parameters

(14) Binstead, R. A.; Meyer, T. J., manuscript in preparation.
(15) Lilie, J.; Beck, G.; Henglein, A. *Ber. Bunsenges. Phys. Chem.* **1971**, *75*, 458.
(16) Stewart, R. *J. Am. Chem. Soc.* **1957**, *79*, 3057. Stewart, R.; Van der Linden, R. *Discuss. Faraday Soc.* **1960**, 211.
(17) Melander, L. C. "Reaction Rates of Isotopic Molecules"; Wiley: New York, 1980.
(18) Keene, F. R.; Young, R. C.; Meyer, T. J. *J. Am. Chem. Soc.* **1977**, *99*, 2468. Brown, G.; Sutin, N. *Ibid.* **1972**, *50*, 2000.
(19) (a) Fuoss, R. M. *J. Am. Chem. Soc.* **1958**, *80*, 5059. (b) Petrucci, S. "Ionic Interactions"; Petrucci, S., Ed.; Academic Press: New York, 1971; Vols. I and II. (c) Eigen, M.; Kruse, W.; Maas, G.; Maeyer, D. L. *Prog. React. Kinet.* **1964**, *2*, 287.
(20) Lee, D. G.; vanden Engh, M. *Can. J. Chem.* **1972**, *50*, 2000.

mentioned above. (2) The fact that rate constants for the oxidation of aromatic hydrocarbons are comparable and even more rapid than the rate constant for 2-propanol[21] even though aromatic hydrocarbons are known to be far less reactive toward one-electron oxidants.[22] (3) Oxidation of cyclobutanol by $Ru(trpy)(bpy)O^{2+}$ gives cyclobutanone as a product[23] whereas one-electron oxidants characteristically give ring-opened oxidation products.[24]

Mechanism of Oxidation by $Ru(trpy)(bpy)O^{2+}$ in Water. There are several ways that a two-electron transfer can occur mechanistically. However, for the reaction studied here some of the possible pathways can be ruled out on the basis of experimental results.

One striking feature of the oxidation is the sizeable β kinetic isotope effect resulting from the deuteration of the methyl groups the 2-propanol: $k_{CH_3}/k_{CD_3} = 3.5$ from Table II. With the assumption that the effects of the deuteration at the separate methyl groups are multiplicative, the isotope effect on a per methyl basis is 1.9. The sizable β isotope effect suggested the possibility that the reaction might proceed in a concerted way involving hydrogen abstractions from both α- and β-positions as shown in eq 20. It

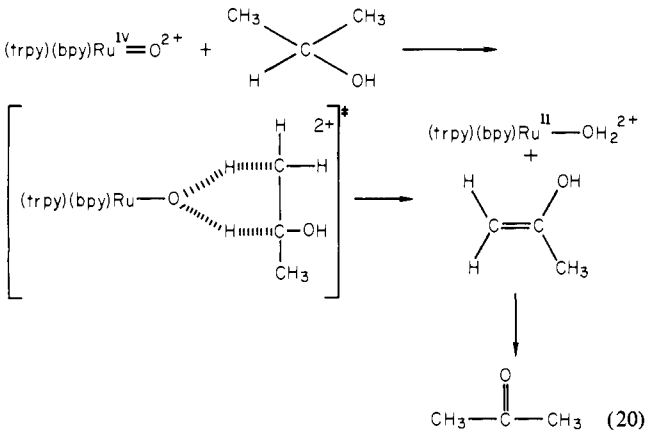

(20)

was possible to rule out hydrogen transfer from the methyl group by carrying out the oxidation of $(CH_3)_2CHOD$ in D_2O. The proton-decoupled ^{13}C NMR spectrum of the acetone product showed only a sharp singlet for the methyl carbon peak. Were the initial organic product the enol as in eq 20, the organic product would have been CH_3COCH_2D because of rapid O–H/O–D exchange in the enol followed by

$$CH_2{=}C(CH_3)OD \rightarrow CH_2DCOCH_3$$

In this case the ^{13}C NMR of monodeuterioacetone would have shown a 1:1:1 triplet for the methyl carbon signal as a result of splitting by the deuteron.

A second possibility to consider is that the reaction proceeds through an initial intermediate involving oxidant–alcohol complex formation. The obvious analogy is with Cr(VI) oxidations where the oxidation of sterically hindered secondary alcohols proceeds through chromate ester formation.[22,25]

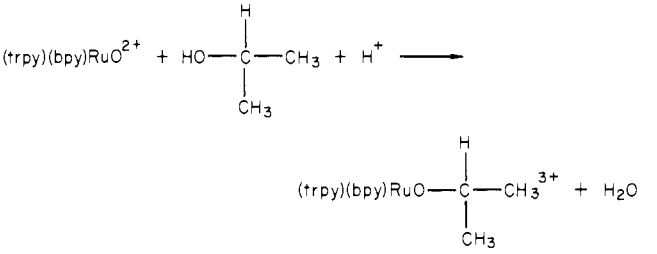

Such a process seems unlikely when the lack of observable intermediates, lack of oxo exchange of the complex with water over a 2-h period,[4] and lack of proton dependence in the rate law is taken into account.

However, metallo ester formation could also occur by coordination sphere expansion to give a seven-coordinate alkoxy–hydroxy complex.

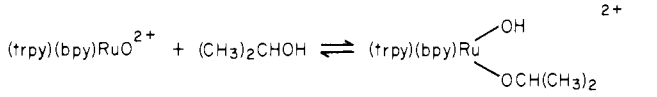

Seven-coordinate complexes of ruthenium(IV) are known.[26] However, for the reaction to be sufficiently facile, it would have to exceed the rate exchange with water. However, as noted above, O-exchange with solvent is slow even though it could proceed by the analogous, seven-coordinate dihydroxy intermediate $(trpy)(bpy)Ru(OH)_2^{2+}$. It is also worthwhile to note that there is no inherent need for the oxidant to function via the formation of a discrete intermediate prior to the redox step. The Ru(IV) oxo complex is known to undergo well-defined reactions with aromatic hydrocarbons at rates comparable to the 2-propanol oxidation.[21]

Even in the absence of the formation of a discrete intermediate, the initial step in the overall reaction must involve the formation of a loosely bound association complex, eq 21, followed by the

$$Ru(trpy)(bpy)O^{2+} + (CH_3)_2CHOH \rightleftharpoons Ru(trpy)(bpy)O^{2+}, (CH_3)_2CHOH \quad (21)$$

$$Ru(trpy)(bpy)O^{2+}, (CH_3)_2CHOH \rightarrow Ru(trpy)(bpy)OH_2^{2+} + (CH_3)_2CO \quad (22)$$

redox step. The thermodynamic quantities K_A, ΔH_A, and ΔS_A which characterize the preequilibrium in eq 21 appear in the experimental kinetic parameters. Their magnitude can be estimated by using known equations as shown below where d is the internuclear separation between reactants in centimeters and N_0 is Avogadro's number.[19]

$$K_A = 4\pi N_0 d^3/3000 = \Delta S_A = R \ln (4\pi N_0 d^3/3000)$$

$$\Delta H_A = -RT/2$$

Assuming average molecular radii of 6.5×10^{-8} cm for $Ru(bpy)_2(py)O^{2+}$ and 3.0×10^{-8} cm for 2-propanol gives $K_A = 2$, $\Delta S_A = 1.5$ eu, and $\Delta H_A = -0.3$ kcal/mol and for the kinetic parameters characterizing the redox step in eq 22

$$k_{IV,redox} = k_{IV}/K_A = 3.4 \times 10^{-2}\ s^{-1}$$

$$\Delta H^{\ddagger}_{IV,redox} = \Delta H^{\ddagger}_{IV} - \Delta H_A = 9\ \text{kcal/mol}$$

$$\Delta S^{\ddagger}_{IV,redox} = \Delta S^{\ddagger}_{IV} - \Delta S_A = -32\ \text{eu}$$

Even accepting that the essential details of the redox step are two electron in nature, there remains something of a mechanistic ambiguity. One of two feasible reaction pathways would involve insertion of the $Ru^{IV}{=}O$ group into the C–H bond, which would give the discrete intermediate shown in eq 23. The second pathway would involve a hydride transfer, eq 24. The hydride

(21) Thompson, M. S.; Meyer, T. J. *J. Am. Chem. Soc.*, in press.

(22) (a) Wiberg, K. B., Ed. "Oxidation in Organic Chemistry"; Academic Press: New York, 1965. (b) Benson, D. "Mechanisms of Oxidation by Metal Ions"; Elsevier: New York, 1976.

(23) Samuels, G., unpublished observations. Actually, the experimental result was somewhat ambiguous. The major product was cyclobutanone but ring-opened products were observed in the solution. The presence of ring-opened products is expected because of the contribution to the overall oxidation of cyclobutanol by $Ru(bpy)_2(py)OH^{2+}$, which is unavoidable in the experiment. Oxidation by Ru(III) appears to be more important for cyclobutanol than for 2-propanol and the oxidation must involve a one-electron transfer step.

(24) Rocek, J.; Radkowsky, A. E. *J. Am. Chem. Soc.* **1973**, *95*, 7123; *J. Org. Chem.* **1973**, *38*, 84. Rocek, J.; Meyer, J. *J. Am. Chem. Soc.* **1972**, *94*, 1209.

(25) Rocek, J.; Westheimer, F. H.; Eschenmoser, A.; Moldovany, L.; Schreiber, J. *Helv. Chim. Acta* **1962**, *45*, 2554.

(26) Wheeler, S. H.; Mattson, B. M.; Pignolet, L. H. *Inorg. Chem.* **1978**, *17*, 340.

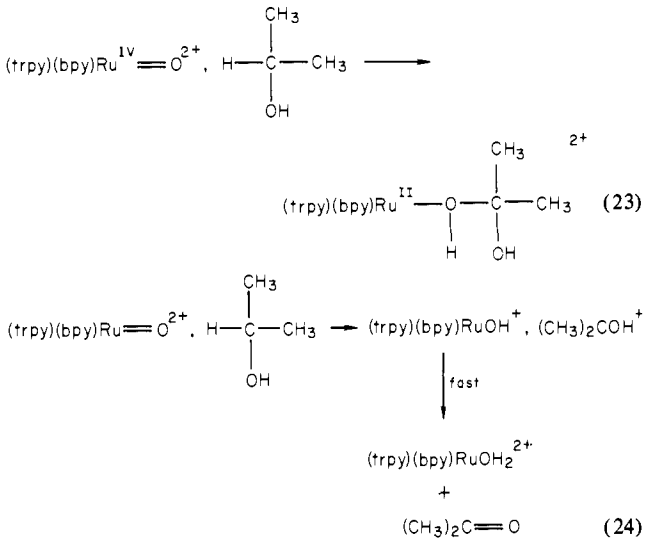

(23)

(24)

transfer could be accompanied by a concerted proton transfer from the hydroxyl group on the alcohol to the oxygen atom of Ru, eq 25. However, the small isotope effect for OH deuteration (Table

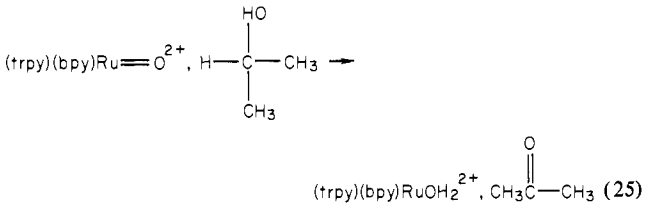

(25)

II) suggests that proton transfer from the hydroxyl group is unimportant in the activation step.

The mechanisms in eq 23 and 24 are related in that both involve net two-electron-transfer steps. The metal is the electron acceptor site in that the acceptor orbitals involved are largely $d\pi$ in character and the oxo site functions as an electronic "lead-in" group to the C–H bond. The mechanisms differ in the net angle of attack of the ruthenyl group on the C–H bond,[27] where for the hydride transfer pathway the net line of attack is end-on (eq 26) and for insertion, side-on (eq 27). In either case, strong wave

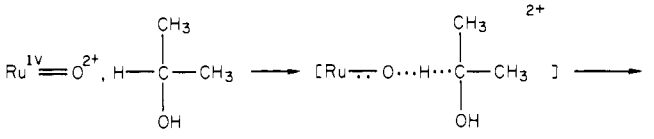

(26)

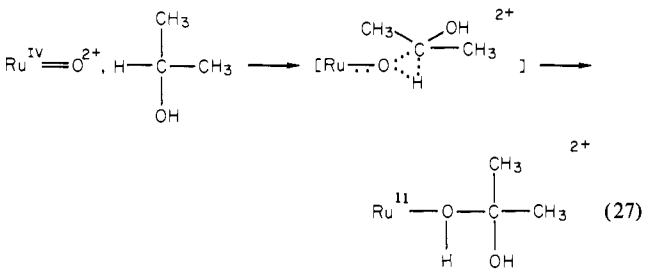

(27)

function mixing between an orbital containing an electron pair on the oxygen of the ruthenyl group and an antibonding, largely α-CH MO of the alcohol must occur as the reaction proceeds along the appropriate energy surface.

The ^{18}O-labeling result shows that oxygen transfer does not occur, which is consistent with hydride transfer. For it to be consistent with insertion requires that eq 28 be fast on the time

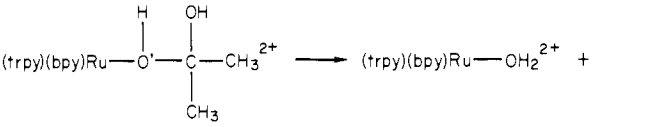

(28)

scale for the redox step since no intermediates are observed in the reaction. The rate constant for dehydration of acetone hydrate is only 10^{-2} s^{-1} at 25 °C,[28] but the dehydration reaction could be greatly accelerated by coordination to the metal ion.

At first glance it would appear that the hydride-transfer mechanism might be untenable energetically because the proton transfer which follows the redox step is favored by 24 kcal/mol on the basis of the pK_a's of protonated acetone[29] and the Ru(II) complex (eq 29).[1] However, as intermediates, the pair Ru-

$$Ru(trpy)(bpy)OH^+ + (CH_3)_2COH^+ \xrightarrow[\Delta G = -24\ kcal/mol]{} Ru(trpy)(bpy)OH_2^{2+} + (CH_3)_2C{=}O \quad (29)$$

$(trpy)(bpy)OH^+ + (CH_3)_2COH^+$ are accessible because ΔG for the redox step is so highly favored. The energetics involved are summarized below.

$$Ru^{IV}(trpy)(bpy)O^{2+} + (CH_3)_2CHOH \rightarrow Ru^{II}(trpy)(bpy)OH^+ + (CH_3)_2COH^+$$

$$\Delta G = -25\ kcal/mol$$

$$Ru^{II}(trpy)(bpy)OH^+ + (CH_3)_2COH^+ \rightarrow Ru^{II}(trpy)(bpy)OH_2^{2+} + (CH_3)_2CO$$

$$\Delta G = -49\ kcal/mol$$

Further Mechanistic Details. A clear distinction between C–H insertion and hydride abstraction pathways is not possible, based on direct evidence. However, the hydride-transfer mechanism is supported by the pattern and magnitude of the kinetic isotope effects. As noted above, the magnitude of the β kinetic isotope effect (1.9/methyl group) arising from the substitution of D for H is relatively large. However, it is in the range found for β deuterium isotope effects in S_N1 solvolysis reactions,[17] and there are expected similarities between hydride transfer and S_N1 reactions, namely, the buildup of positive charge and the sense of the rehybridization at the carbon center.

There is an additional point to be made about the kinetic isotope effects. In the high-temperature, semiclassical limit, reaction rate theory predicts that zero-point energy effects will be the dominant origin of kinetic isotope effects. In this region an appreciable secondary isotope effect can only be expected where there are significant changes in vibrational structure between reactants and the activated complex.[17] Although the applicability of high-temperature limit arguments is not clear, the criterion developed above based on structural changes is clearly not met by the C–H insertion mechanism where there is no real change in hybridization at the central carbon atom. The hydride abstraction mechanism fits this criterion quite well.

If the hydride transfer mechanism is operative, the absence of a significant ionic strength effect on the oxidation by Ru(IV) is significant. It would seem unavoidable that the critical phase in the oxidation is in the initial stage of the reaction and the interaction between an electron pair on the oxo group and σ^*(C–H) before significant charge transfer has occurred.

In summary, the picture that emerges for the Ru(IV) oxidation of 2-propanol is a two-electron, hydride-transfer mechanism as shown in eq 26. The activational process must involve in a critical way both α-C–H and Ru–O vibrations and, to a lesser degree, normal coordinates involving the methyl groups. The relatively

(27) More O'Farrell, R. A. *J. Chem. Soc. B* **1970**, 785.

(28) Bell, R. P. *Adv. Phys. Org. Chem.* **1966**, *4*, 1.

(29) Streitweiser, A.; Heathcock, C. H. "Introduction to Organic Chemistry"; MacMillan, New York, 1976.

small energy of activation (3200 cm^{-1}) shows the importance of strong electron-vibrational coupling which is critically dependent upon the extent of α-C–H bond stretching toward the Ru–O electron acceptor site. Given the suggested mechanism, contributions to $\Delta S^{\ddagger}$ are expected to arise from the following: (1) Specific orientational demands between the reactants associated with "aligning" the $Ru{=}O^{2+}$ and H–C groups in the association complex. (2) Quantum mechanical vibrational overlap or "nuclear tunneling" effects.

Mechanisms of Oxidation in Acetonitrile. Accessibility of Multiple Pathways. The oxidations of 2-propanol by Ru(trpy)(bpy)O^{2+} in water or by $Ru(bpy)_2(py)O^{2+}$ in acetonitrile appear to occur by the same mechanism as suggested by the lack of oxo transfer and the similarities between activational parameters and H/D kinetic isotope effects. Solvent effects[30] should play a role in determining the energy barrier for hydride transfer since as in an outer-sphere reaction like

$$Ru(trpy)(bpy)OH^{2+},\ (CH_3)_2CHOH \rightarrow Ru(trpy)(bpy)OH^{+},\ (CH_3)_2CHOH^{+}$$

there is a net charge-transfer component in the redox step.

$$Ru{=}O^{2+},\ (CH_3)_2CHOH \rightarrow Ru{-}OH^{+},\ (CH_3)_2COH^{+}$$

The case of oxidation by Ru(III) is much more intriguing. In acetonitrile, oxidation by $Ru(bpy)_2(py)OH^{2+}$ assumes a pattern of isotope effects and activation parameters which are distinctly different from those for oxidation by Ru(trpy)(bpy)OH^{2+} in water. In acetonitrile there are considerable decreases in both $\Delta H^{\ddagger}$ and $\Delta S^{\ddagger}$ and the magnitudes of the values are reminiscent of those obtained for the oxidation by Ru(IV). The reaction must still be one electron in nature, and a change in mechanism from outer-sphere (eq 15) to proton-coupled electron transfer (eq 17) is unlikely because of the small OH/OD kinetic isotope effect (Table III). The remaining possibility is a transition between outer-sphere electron transfer and H-atom transfer (eq 16), induced by the change in solvents. If the latter explanation is correct, the origin of the relatively small $\Delta H^{\ddagger}$ and negative $\Delta S^{\ddagger}$ values would also be in the strong electron-vibrational coupling, specific orientational demands, and quantum mechanical nuclear tunneling expected for H atom transfer.

Conclusions and Final Comments

The results obtained here can be satisfactorily interpreted in terms of two-electron oxidation pathways for the oxidation of 2-propanol by the Ru(IV) oxo complexes and one-electron oxidation pathways for the Ru(III) hydroxy complexes. For the Ru(IV) reactions the most likely mechanism is a concerted hydride transfer from the α-C–H bond of 2-propanol to the oxo group which serves as a lead-in atom to the Ru(IV) electron acceptor site. The oxo group is not transferred to the substrate, and in that sense the reaction occurs by a template mechanism. This is an important observation for what it reveals about the use of Ru(IV) oxo and related complexes in catalytic redox applications. Since metal–ligand bonds are not broken in the reaction, even substitutionally inert second- and third-row transition-metal complexes are capable of sustaining catalysis under conditions where the rate-limiting steps will be based on redox rather than substitutional chemistry.

Our observations may also presage the development of or help explain the basis of operation for existing catalytic redox systems based on groups such as M=NR or M=S. They may also provide a basis for the development of reductive catalysts using the same mechanism but operated in the reverse direction based on microscopic reversibility.

For the oxidations by Ru(III), the most significant observation is the apparent change in mechanism between water and acetonitrile. What this observation suggests is that Ru(III) and no doubt Ru(IV), where mechanistic diversity has already been established,[1-5,21] have available a variety of accessible redox pathways. It is possible that the dominant pathway for a particular reaction may become predictable and controllable by making systematic changes in such variables as temperature, medium, ΔG, or the substrate itself.

Acknowledgment is made to the National Science Foundation under Grant No. CHE-8002433 for support of this research.

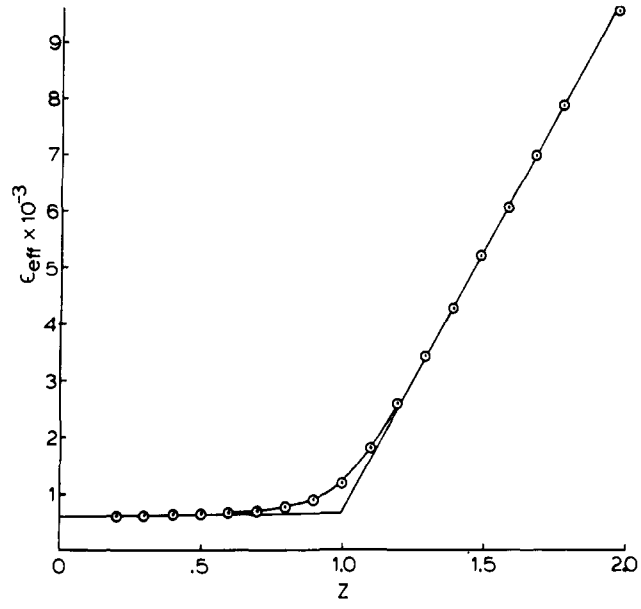

Figure 5. Variation of ϵ_{eff} with the extent of reduction of Ru(trpy)(bpy)O^{2+} at 25 °C in water. Monitoring wavelength is 477 nm.

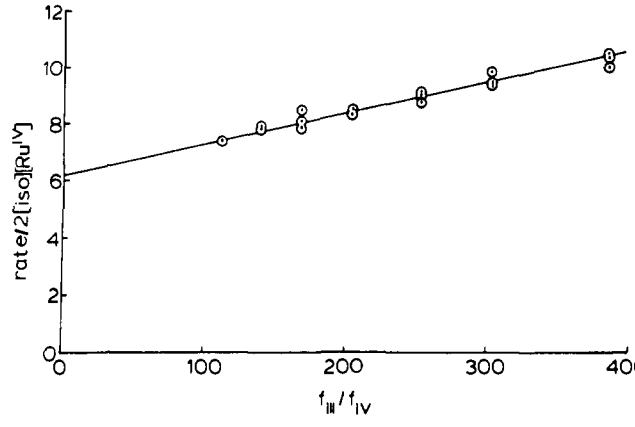

Figure 6. Plot of $(dx/dt)/f_{IV}[S]$ vs. f_{III}/f_{IV} at 477 nm for a kinetic run in the oxidation of 2-propanol by Ru(trpy)(bpy)O^{2+} and Ru(trpy)(bpy)OH^{2+}.

Appendix

Data Treatment for the Oxidation of 2-Propanol by Ru(trpy)(bpy)O^{2+} in Water. As mentioned in the body of the paper, spectral studies show that the oxidation of 2-propanol by Ru(trpy)(bpy)O^{2+} occurs in three separate stages. In the first, oxidation is dominated by Ru(IV), in the second the oxidation is still dominated by Ru(IV) but the oxidation step is preceded by disproportionation of Ru(III) into Ru(II) and Ru(IV), and in the third stage oxidation is dominated by Ru(III).

The total rate at any point during the reaction is given by eq A1, where [S] is the concentration of 2-propanol. Because of the

$$\text{rate} = k'_{IV}[Ru(IV)][S] + k'_{III}[Ru(III)][S] \qquad (A1)$$

complication arising from the fact that a rapid disproportionation interrelates [Ru(IV)] and [Ru(III)], the two terms in eq A1 are not separable for measurement purposes.

Figure 5 shows the effective extinction coefficient (ϵ_{eff}) at 477 nm for the ruthenium system as a function of extent of reduction of the starting Ru(IV) complexes generated by electrochemical

(30) Sullivan, B. P.; Curtis, J. C.; Kober, E. M.; Meyer, T. J. *Nouv. J. Chim.* **1980**, *4*, 643–650.

reduction. Here, z is defined as the number of electrons added per ruthenium. In a 1-cm cell, ϵ_{eff} at a defined wavelength is given by eq A2, and in eq A3 in terms of the extinction coefficients and

$$\epsilon_{eff} = \text{absorbance}/[\text{Ru}](\text{total}) \quad \text{(A2)}$$

mole fractions (f) of the component absorbing species, Ru(II), Ru(III), and Ru(IV).

$$\epsilon_{eff} = f_{II}\epsilon_{II} + f_{III}\epsilon_{III} + f_{IV}\epsilon_{IV} \quad \text{(A3)}$$

$$f_x = [\text{Ru}(x)]/[\text{Ru}(\text{total})]$$

At 477 nm

$\epsilon_{II} = 9600\ M^{-1}\cdot cm^{-1}$; $\epsilon_{III} = 620\ M^{-1}\cdot cm^{-1}$; $\epsilon_{IV} = 600\ M^{-1}\cdot cm^{-1}$

Equations A4 through A6 follow from definitions already given.

$$f_{II} + f_{III} + f_{IV} = 1 \quad \text{(A4)}$$

$$200 = K = f_{III}^2/f_{II}f_{IV} \quad \text{(A5)}$$

$$2f_{II} + f_{III} = z \quad \text{(A6)}$$

Using eq A2 through A6 and the plot of Figure 5, the experimentally obtained absorbance vs. time curves can be converted into z vs. time curves, which give the normalized extent of reduction vs. time. In terms of z, the rate equation is given by eq A7. The factors of 2 in eq A7 take into account the stoichiometries of the oxidations by Ru(III) and Ru(IV). dz/dt is readily obtainable at any time from the slope of the z vs. time plot. Slopes were determined either by computer calculation or by visual estimate by using a ruler without a noticeable difference in results. Rearrangement of eq A7 gives eq A8, which predicts that plots

$$dz/dt = 2k_{IV}f_{IV}[S] + 2k_{III}f_{III}[S] \quad \text{(A7)}$$

$$(dz/dt)/(f_{IV}[S]) = 2k_{IV} + dk_{III}(f_{III}/f_{IV}) \quad \text{(A8)}$$

of $(dz/dt)/f_{IV}[S]$ vs. f_{III}/f_{IV} should yield straight lines of slope $2k_{III}$ and intercept $2k_{IV}$. f_{III} and f_{III}/f_{IV} were calculated from the absorbance vs. time curve using eq A2 through A6. In Figure 6 is shown an actual plot of experimental data plotted as suggested by eq A8.

Straight lines were fitted to data points using a simple linear least-squares program and a Texas Instruments 59 programmable calculator. Each reported rate constant was determined from the average of at least 18 measurements. Experimental uncertainties were estimated from the manufacturer's reported error limits and the scatter observed in a series of measurements on a given system.

Registry No. Ru(trpy)(bpy)O^{2+}, 73836-44-9; Ru(trpy)(bpy)OH^{2+}, 81971-63-3; Ru(bpy)$_2$(py)O^{2+}, 76582-01-9; Ru(bpy)$_2$(py)OH^{2+}, 75495-07-7; $(CH_3)_2CHOH$, 67-63-0.

Weak Metal–Metal Bonds in an "Electron-Rich" Cluster. The Synthesis and X-ray Crystallographic Characterization of $Os_4(CO)_{12}(\mu_3\text{-}S)_2$ and $Os_6(CO)_{16}(\mu_4\text{-}S)(\mu_3\text{-}S)$

Richard D. Adams* and Li-Wu Yang

Contribution from the Department of Chemistry, Yale University, New Haven, Connecticut 06511. *Received December 7, 1981*

Abstract: The thermal decomposition of $HOs_3(CO)_{10}(\mu\text{-SPh})$ in refluxing nonane leads to the elimination of benzene and formation of the known sulfidoosmium carbonyl clusters $H_2Os_3(CO)_9(\mu_3\text{-S})$ (**1**) and $Os_3(CO)_9(\mu_3\text{-S})_2$ (**2**) in addition to the new higher nuclearity clusters $Os_4(CO)_{12}(\mu_3\text{-S})$ (**3**), $Os_4(CO)_{12}(\mu_3\text{-S})_2$ (**4**), and $Os_6(CO)_{16}(\mu_4\text{-S})(\mu_3\text{-S})$ (**5**). The molecular structures of **4** and **5** were established by X-ray crystallographic methods; for **4**, space group $P\bar{1}$; $a = 8.491$ (2) Å; $b = 9.240$ (2) Å; $c = 14.389$ (5) Å; $\alpha = 80.54$ (2)°; $\beta = 85.94$ (2)°; $\gamma = 68.31$ (5)°; $Z = 2$, $\rho_{calcd} = 3.728$ g/cm^3. The structure was solved by the heavy-atom method. Least-squares refinement on 2930 reflections ($F^2 \geq 3.0\sigma(F^2)$) produced the final residuals $R_1 = 0.032$ and $R_2 = 0.034$. **4** contains a butterfly cluster of four osmium atoms with sulfido ligands bridging the two open triangular faces and three carbonyl ligands on each metal atom. Electron counting shows that **4** is a 64-electron cluster and and thus should contain only four metal–metal bonds. However, the structural analysis shows the existence of five metal–metal bonds, although two are significantly elongated with internuclear separations of 3.091 (1) and 3.002 (1) Å. The relationship of the bonding in this cluster to current theories of cluster bonding is described and discussed. For **5**, space group $P2_1/c$; $a = 10.083$ (4) Å; $b = 12.633$ (4) Å; $c = 21.383$ (4) Å; $\beta = 91.73$ (2)°; $Z = 4$, $\rho_{calcd} = 4.03$ g/cm^3. The structure was solved by a combination of direct methods (MULTAN) and difference-Fourier techniques. Least-squares refinement on 2629 reflections ($F^2 \geq 3.0\sigma(F^2)$) produced the final residuals $R_1 = 0.038$ and $R_2 = 0.039$. The structure of **5** contains a square-pyramidal cluster of five osmium atoms with a quadruply bridging sulfido ligand spanning the square base. The sixth metal atom bridges two metal atoms in the square base, and this group of three is capped by a triply bridging sulfido ligand. Sixteen linear carbonyl ligands cover the "surface" of the cluster.

The electronic structures and bonding in transition-metal cluster complexes are currently a topic of great interest and importance, but it is one that also lacks a fully uniform explanation.[1] The bonding in clusters containing up to four metal atoms can usually be explained through the traditional two-center–two-electron bonding model.[1-3] In higher nuclearity polyhedral clusters, molecular orbital treatments have successfully explained irregular electron counts.[1-6] As one might expect, there may be a family of important molecules that does not fall readily into either class. We have now synthesized the cluster compound $Os_4(CO)_{12}(\mu_3\text{-S})_2$ and feel that it may be a prototype for such anomalous clusters.

We have found that the thermal decomposition of (arenethiolato)osmium carbonyl hydride clusters provides a new route

(1) Wade, K. in "Transition-Metal Clusters"; Johnson, B. F. G., Ed.; Wiley: New York, 1980.
(2) Johnson, B. F. G.; Benfield, R. E. *Top. Stereochem.* **1981**, *12*, 253.
(3) Mingos, D. M. P. *Nature (London), Phys. Sci.* **1972**, *236*, 99.
(4) Wade, K. *Adv. Inorg. Chem. Radiochem.* **1976**, *18*, 1.
(5) Mingos, D. M. P. *J. Chem. Soc., Dalton Trans.* **1974**, 133.
(6) Lauher, J. W. *J. Am. Chem. Soc.* **1978**, *100*, 5305.

0002-7863/82/1504-4115$01.25/0